

Substrate suppression of oxidation process in pnictogen monolayers

Rafael L. H. Freire¹,* F. Crasto de Lima¹,† and A. Fazzio¹,‡
Ilum School of Science, CNPEM, 13083-970, Campinas, SP, Brazil

(Dated: July 4, 2023)

2D materials present an interesting platform for device designs. However, oxidation can drastically change the system's properties, which need to be accounted for. Through *ab initio* calculations, we investigated freestanding and SiC-supported As, Sb, and Bi mono-elemental layers. The oxidation process occurs through an O₂ spin-state transition, accounted for within the Landau-Zener transition. Additionally, we have investigated the oxidation barriers and the role of spin-orbit coupling. Our calculations pointed out that the presence of SiC substrate reduces the oxidation time scale compared to a freestanding monolayer. We have extracted the energy barrier transition, compatible with our spin-transition analysis. Besides, spin-orbit coupling is relevant to the oxidation mechanisms and alters time scales. The energy barriers decrease as the pnictogen changes from As to Sb to Bi for the freestanding systems, while for SiC-supported, they increase across the pnictogen family. Our computed energy barriers confirm the enhanced robustness against oxidation for the SiC-supported systems.

The realization of two-dimensional (2D) materials through diverse experimental techniques have increased interest in their technological applications on electronic devices. Particularly, the arising topological insulating phase in bismuthene [1], antimonene [2], strained arsenene [3, 4], with the former robust against disorder [5, 6], leading to low-power spintronics [7]. However, the experimental conditions towards scalable production of these materials pose great challenges due to their relatively low stability [8], mainly at room temperature and in the presence of air (oxygen). Freestanding mono-elemental materials, like phosphorene, were shown to be very unstable upon O₂-exposure being degraded within a few hours [9]. Indeed, freestanding monolayer pnictogens (P and As) are more prone to oxidation than other 2D materials presenting the same atomic structure [10], while the presence of a substrate can alter the oxidation process [8].

The O₂ molecule occurs naturally in a triplet ($^3\Sigma_g^-$) ground state. On the other hand, under experimental conditions (e.g., photoexcitation [11]), O₂ molecule can be found in excited singlet states, namely $^1\Delta_g$ and $^1\Sigma_g^+$. The singlet states are more reactive than the ground state triplet, being of great importance in oxidation process [12]. Experimental results over oxidation of 3D-stacked pnictogen systems (down to a few layers), show the robustness of oxidation for the internal layers, while the surface presents oxygen groups [13, 14]. Ruled by the higher interlayer bond of heavier pnictogens (compared with the phosphorene), the formation of surface oxide-layer protects the internal layers from oxidation [15–17]. There are studies about oxidation on 2D pnictogen materials, however focusing on the freestanding configuration [18–23], while not taking into account fundamental aspects, such as the role of triplet-singlet transitions, and spin-orbit effects.

At the same time, the realization of supported materials through molecular beam epitaxy (MBE) has attracted attention, for example, Sb/Ag(111) [24], Bi/SiC(0001) [25] and As/SiC(0001) [26] with a planar structure [27].

Particularly, the topological insulating phase of bismuthene and other pnictogens was predicted when supported on SiC substrate [1, 2]. While the presence of a substrate can alter the oxidation kinetics of 2D systems [28]. In this sense, understanding the mechanisms behind oxygen interaction with those substrate-supported materials is a key point for future experimental investigations upon applications and routes to improve their stability.

In this paper, we show that the oxidation process of pnictogen monolayers is considerably lower (slower) when deposited on top of SiC substrate. Taking an *ab initio* approach based on the density functional theory (DFT) we investigated the rate of formation of reactive oxygen species, i.e. O₂ triplet-singlet transition, close to the materials' surface in the buckled free-standing (FS) form and in the flat structure when on top of SiC substrate (SiC). We connected such rate of formation with the reaction barrier calculated within the nudge elastic band (NEB) method. The FS case reacts barrierless with the singlet O₂ molecule, while the supported one presents a non-negligible barrier. Additionally, the barriers found for the triplet O₂ molecule are considerably larger for the heavier pnictogen Bi. Our results draw attention to the possible atmospheric stability of supported pnictogens monolayer.

Group-5A elemental monolayers were investigated through spin-polarized calculations based on density functional theory (DFT) [29, 30], performed within the semi-local exchange-correlation functional proposed by Perdew–Burke–Ernzerhof [31]. For the total energies, the electron-ion interactions were considered within the projector augmented wave (PAW) method [32, 33], as implemented in the vienna *ab-initio* simulation package (VASP) [34, 35]. For all calculations, the cutoff energy for the plane-wave expansion of the Kohn–Sham orbitals was set to 400 eV, under an energy convergence parameter of 10⁻⁶ eV, with all atoms relaxed until the atomic forces on every atom were smaller than 10⁻² eV Å⁻¹. We considered 3 × 3 unit cells with 13 Å and 16 Å distance between periodic images for FS and SiC-supported sys-

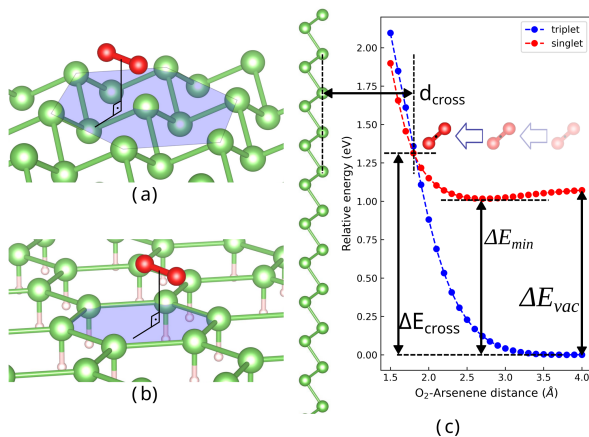


FIG. 1. O_2 adsorption model for (a) freestanding and (b) SiC-supported structures, and (c) an example for evaluating the Landau-Zener probabilities, including a few definitions like the distance of the molecule center-of-mass from the 2D material surface at the triplet-singlet crossing (d_{cross}), the singlet-triplet energy difference far from the surface (ΔE_{vac}), at the energy minimum (ΔE_{min}).

tems respectively. A uniform $4 \times 4 \times 1$ k-point mesh was considered for the Brillouin zone (BZ) integration.

The oxidation process of pnictogen 2D allotropes is known in the literature to be an exothermic process. We calculate the adsorption energy (E_a) of a single oxygen atom on the pnictogen surface in its buckled freestanding geometry (FS) and in the flat geometry presented when supported on silicon-carbide (SiC-supported) [Fig. 1(a) and (b)]. It is worth pointing out that the bismuthene and antimonene on top of SiC form honeycomb lattices, while arsenene has a lower energy triangular lattice [26], which is considered here. In Table I, we present our calculations for the adsorption energy

$$E_a = E_{X+O} - E_X - \frac{1}{2}E_{O_2}, \quad (1)$$

where E_X is the pristine pnictogen configuration, E_{X+O} the pnictogen with single oxygen adsorbed on its surface, and E_{O_2} the isolated O_2 molecule total energy. Indeed, the adsorption process is still exothermic even for the substrate-supported case. To obtain those adsorption energies we have considered different adsorption sites according to the surface geometry. Thus, in the FS case, we probed on-top, bridge, valley, and hollow sites, while for SiC were on-top, bridge, and hollow sites. For all cases in the lower energy configuration, the oxygen atom forms a bridge between adjacent pnictogen atoms. Comparing the FS with the supported SiC system, we see higher adsorption energies for Sb and Bi, while a decrease is observed for As. Here, the supported As system has a larger tensile strain than the Sb and Bi, when compared to their freestanding structure [26]. The oxygen adsorption, bridging two adjacent As atoms, contributes to lowering the tensile strain, therefore leading to lower adsorption energy.

TABLE I. Oxygen adsorption energy, E_a (eV/O-atom), on pnictogen surfaces on their freestanding (FS) configuration and on silicon carbide-supported (SiC) configuration. The most stable configuration is an epoxy-like bridge bond inclined towards the hexagonal center.

phases	As	Sb	Bi
FS	-1.01	-1.32	-1.06
SiC	-2.69	-1.15	-0.45

Although there is an indication of a higher exothermic process for As, oxidation can have different reaction time scales for each system. Here we will (i) explore the Landau-Zener probability of transition between oxygen molecule triplet and its most reactive form, oxygen-singlet, close to the pnictogen surfaces and (ii) explore energy barriers for the oxidation process considering the role of the spin-orbit coupling through the nudge elastic band (NEB) method.

Analyzing the total energy of an O_2 molecule close to a materials interface, we see a dependence between the singlet and triplet spin configurations total energies and the molecule distance from the pnictogen surface, as show in Fig. 1 (c). Away from the surface the singlet and triplet state are separated in energy by $\Delta E_{vac} \sim 1$ eV, while close to the pnictogen surfaces they present an energy crossing. This crossing implies a transition probability between the two spin states of O_2 molecule. Based on the slope of the triplet and singlet curves we have obtained the triplet-singlet transition probabilities (P_{ts}) by employing the Landau-Zener relation (P_{LZ}) [8, 36, 37]

$$P_{ts} = (1 - P_{LZ})(1 + P_{LZ}), \quad (2)$$

where

$$P_{LZ} = \exp\left(-\frac{V^2}{\hbar v |F_t - F_s|}\right). \quad (3)$$

Here, V is the spin-orbit matrix element of O_2 molecule (122 cm^{-1}), v the velocity of O_2 molecule at room temperature (483.59 m s^{-1}), and F_i the forces acting on the O_2 molecule for each spin state (triplet and singlet) [8]. It is worth noting that F_i will depend on the materials local adsorption site, and the arriving geometry of the O_2 molecule. That is, a single adsorption site can not capture the variations on triplet-single transition, as at experimental conditions this should run over a large distribution of possible sites and molecule geometries (orientation with respect to the surface). Our analysis includes different adsorption sites for both FS and SiC-supported structures and different molecule geometries. This will generate one-dimensional curves as that presented as an example in Fig. 1 (c), in which the singlet and triplet potential energy surfaces cross at some point (d_{cross}) [37]. We extracted information about the (i) triplet-singlet crossing distance (d_{cross}); (ii) crossing point relative energy (ΔE_{cross}), (iii) the singlet minimum relative energy

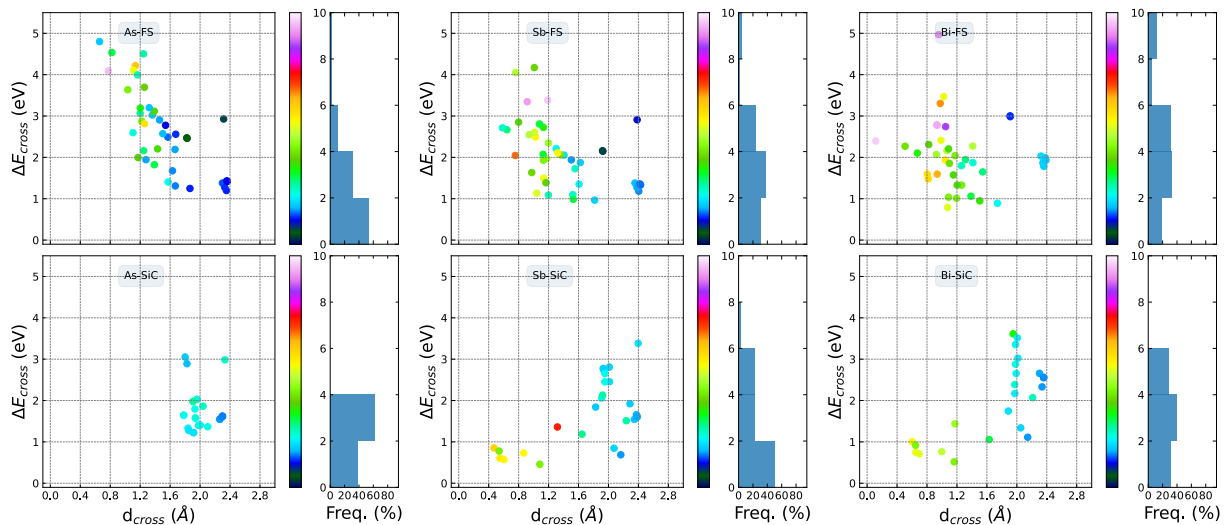


FIG. 2. Triplet-singlet Landau-Zener transition probabilities (P_{ts}) for free-standing (top) and SiC-supported (bottom) systems for a few different adsorption sites, depicted with the triplet-singlet crossing distance (d_{cross}) and crossing energy (ΔE_{cross}). P_{ts} is indicated by the color bar, and the histogram indicates the P_{ts} value distribution.

(ΔE_{min}), and (iv) the triplet-singlet transition probability (P_{ts}).

In Fig. 2, we present the triplet-singlet transition probability (P_{ts} , in the color bar), mapping it with respect to the crossing relative energies (ΔE_{cross}) and the distance from the surface at the crossing point (d_{cross}). In the right panel close to the color bar we represent the P_{ts} statistical distribution. Here, 50% of the FS configurations presented P_{ts} 's $< 5\%$, while 60% for SiC-supported. Additionally, the SiC-supported has a probability transition more concentrated around the 2%, while the FS configurations present values spreading to higher probabilities. That is, we have a statistical indication that the triplet-single transition is more probable in FS than in the SiC-supported pnictogens.

In Table II, we summarize the average values and mean deviation for the different configurations probed. Despite the significant mean deviation values, we can see that the P_{ts} average for FS is larger than that for SiC-supported, indicating FS as more prone to O_2 triplet-singlet transition than SiC-supported, thus facilitating the oxidation process. The crossing distance between the triplet-singlet curves is higher for the SiC-supported than in FS, given the buckled nature of the latter. We see a monotonic growth of P_{ts} when going from As \rightarrow Sb \rightarrow Bi in the FS case, which is not observed for the SiC system. Furthermore, we see a correlation between d_{cross} with the P_{ts} , where the closer to the surface, the larger P_{ts} , that is, the surface orbitals interaction with the molecule is ruling the transition. In fact, because of the different bonding nature within the two structures, their orbitals will have different spreading into the vacuum region. In the FS structure, there is a hybridization between in-plane and out-of-plane orbitals forming a sp^3 (s, p_x, p_y, p_z) bonding, while in the flat SiC-supported, the absence of hybridiza-

TABLE II. Average values of ΔE_{min} (eV), d_{cross} (Å) [shown in Fig. 1], and Landau-Zener triplet-singlet probability transition P_{ts} (%) for all configurations tested [Fig. 2]. Numbers in parentheses are the standard deviation for the respective quantity.

phases		ΔE_{min}	d_{cross}^{OCM}	P_{ts}
As	FS	1.04 (0.02)	1.51 (0.46)	2.46 (1.78)
	SiC	0.94 (0.11)	1.87 (0.28)	2.15 (1.25)
Sb	FS	0.93 (0.07)	1.41 (0.54)	3.33 (2.03)
	SiC	0.72 (0.15)	1.74 (0.64)	2.85 (1.67)
Bi	FS	0.77 (0.09)	1.30 (0.55)	4.25 (2.31)
	SiC	0.70 (0.10)	1.74 (0.61)	2.77 (1.34)

tion between in-plane and out-of-plane orbitals leads to the formation of a sp^2 bonding, and a remaining out-of-plane orbital (p_z) [27]. Because the p_z orbital is not hybridized in the latter it can possibly spread into larger distances within the vacuum region if compared to the FS structure. Thus, the molecule will feel the presence of the SiC-supported structure at larger distances as a result of the interaction with this out-of-plane orbital depending on the surface site and geometry it approaches. The singlet configuration presents minimum energy when close to the system surface, being the singlet minimum relative energy (ΔE_{min}) lower for the SiC system. This singlet minimum energy is due to unstable physisorbed configurations of the O_2 that arise only when constraining the system in the singlet state. As we will show below, such configuration presents a barrierless transition to oxidation and cannot be stabilized on FS systems.

Given the scenario for triplet-singlet transition, the reaction rate is also dependent on the energy barrier for both configurations to adsorb on the pnictogen surface.

Here we have calculated the energy barrier through the nudge elastic band (NEB) method, considering three scenarios: (i) O_2 in an enforced singlet configuration, (ii) O_2 with a free spin degree of freedom without spin-orbit coupling, and (iii) a fully relativistic case taking spin-orbit coupling into account. Our results are presented in Fig. 3 and summarized in Table III. First, analyzing the enforced singlet case the O_2 molecule finds no energy barrier to dissociate over the FS material surface, while for SiC-supported systems there always exists an energy barrier. The singlet energy barrier for the latter is lower for the As and Sb system (0.36 and 0.47 eV respectively) while a higher value of 1.52 eV was found for Bi. We see a different scenario when considering a free spin degree of freedom, here far from the surface the O_2 is in a triplet state while through the barrier it changes to a singlet state before dissociation (see the magnetization in the lower panels of Fig. 3). Such behavior is present with or without the spin-orbit effect. This spin transition before the dissociation is dictated by a spin selection rule given the non-magnetic character of oxidized pnictogens [38, 39]. The spin-orbit effect is negligible for As and Sb systems, while presenting different effects on Bi. For Bi-FS the spin-orbit coupling lowers both the barrier maximum and the initial state energies, while for Bi-SiC it lowers the initial state keeping the barrier maximum energy. In the singlet states $s=0$, the spin-orbit contribution vanishes ($\vec{L} \cdot \vec{s}$), while on the triplet state it presents a non-vanishing contribution. For the Bi-FS the triplet state persists higher on the barrier which gives this barrier lowering, while on the Bi-SiC in the barrier maximum, the $s=0$ state is already defined.

We see different behavior of the barrier for FS and SiC configuration across the pnictogen group. While for FS, heavier pnictogen present a lower barrier, for supported system the opposite is observed. The decrease in barrier towards heavier pnictogens in FS configuration was also previously observed [21]. For FS system, the Bi system presents a lower energy barrier. Indeed, our Landau-Zener transition probability analysis has shown that the triplet-singlet transition for Bismuth is more favorable than Sb and As. As indicated by the magnetization panels of Fig. 3, the barrier height in the non-strained FS system is ruled by the triplet-singlet transition. On the other hand, the SiC-supported pnictogens are under strain, which can change their interaction energy with O_2 . Bismuth has the largest atomic radius among the pnictogens studied, being under lower strain followed by Sb and As for the SiC supported structure [26]. Such lower strain energy makes the initial configuration (before O_2 reaction) lower in energy compared with other pnictogens, leading to a higher barrier for the reaction.

The rate of oxidation for the pristine pnictogen systems can be estimated as

$$f_0 = \nu e^{(-E_b/kT)} \quad (4)$$

with ν the attempt frequency, E_b the calculated barrier energy. In the kinetic theory of gases, for one atmospheric

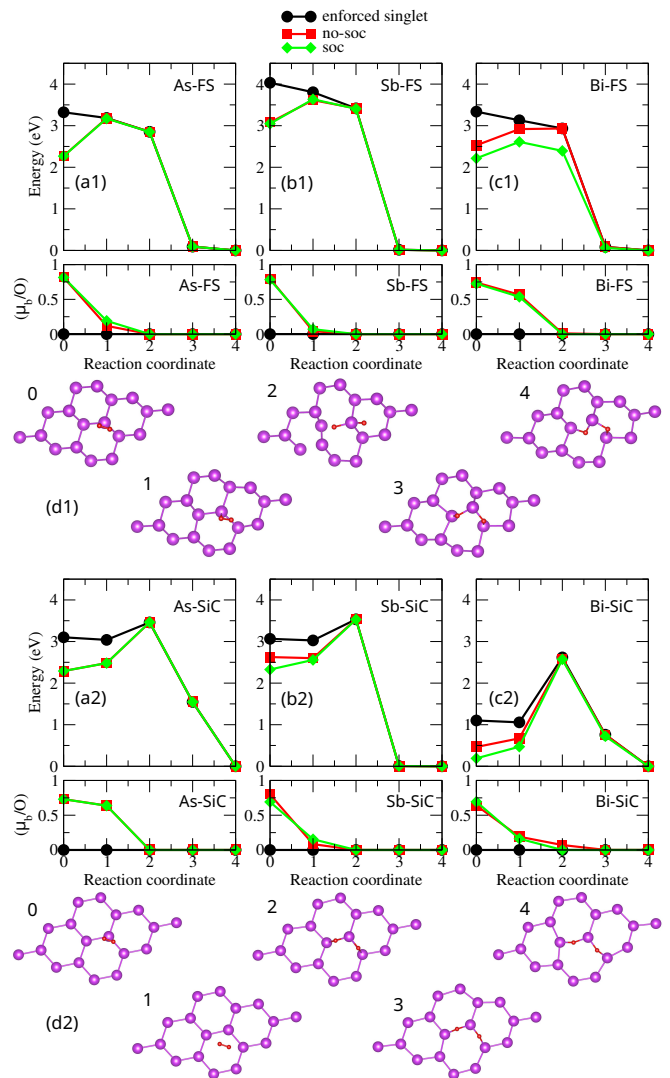


FIG. 3. O_2 reaction barriers (upper panels) and magnetization along the barrier (lower panels) calculated by the nudge elastic band method, for (a1)-(d1) the FS configuration and (a2)-(d2) the SiC configuration. The atoms' trajectory shown is for the Bi systems, similar geometries are observed for the other systems.

pressure, at 300 K ($kT = 0.026$ eV), the number of O_2 molecules arriving at a surface per unity of area, per unity of time is

$$\frac{n}{4} \sqrt{\frac{8kT}{\pi m}} \sim \frac{1.87 \cdot 10^{24}}{s \cdot cm^2}, \quad (5)$$

with $n = 5.1 \cdot 10^{24} m^{-3}$ the number of O_2 molecules in air per volume at atmospheric pressure/temperature, and $m = 4.9 \cdot 10^{-26}$ kg the O_2 mass, at $kT = 4.16 \cdot 10^{-18}$ kg m² s⁻².

Such rate of oxidation f_0 , is valid for the pristine non-oxidized surface. When the system approaches its most stable oxide phase X_2O_3 (with X=As, Sb, Bi), such rate should vanish. Therefore the rate of oxidation should

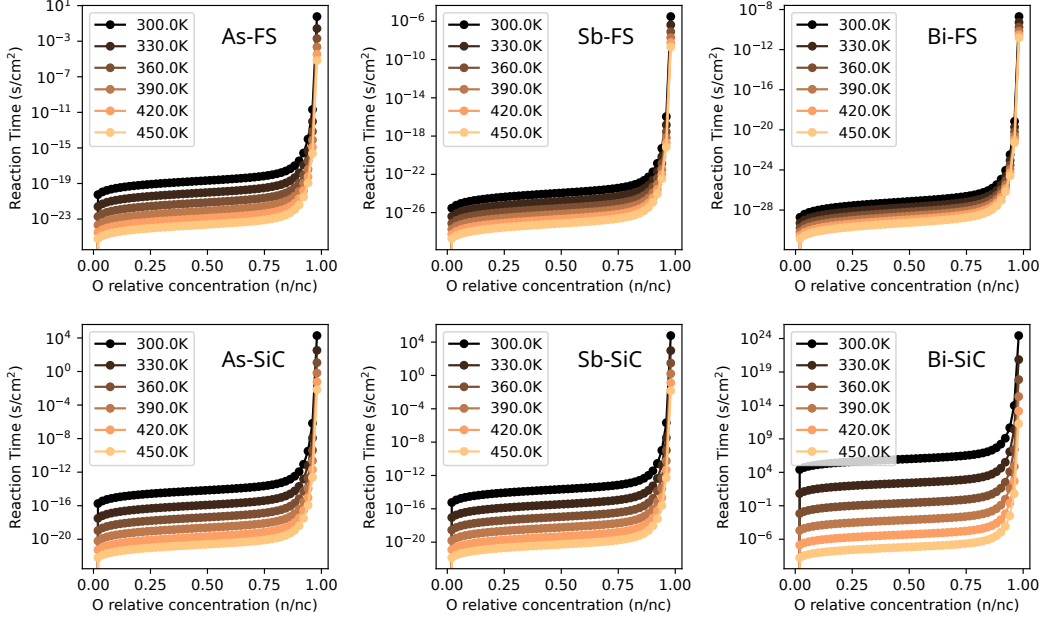


FIG. 4. Reaction time for oxidation from zero up to oxygen concentration of X_2O_3 phase ($X=As, Sb, Bi$), namely critical concentration n_c . Upper panels are for FS configuration and lower panels for SiC-supported.

TABLE III. Barrier energies E_{bar} (eV) for O_2 reaction on pnictogen surfaces for the initial state in enforced singlet ($s = 0$), and triplet ($s = 1$) without/with SOC (no-soc/soc).

system	FS $_{soc}^{s=1}$	FS $_{no-soc}^{s=1}$	FS $^{s=0}$	SiC $_{soc}^{s=1}$	SiC $_{no-soc}^{s=1}$	SiC $^{s=0}$
As	0.90	0.91	0.00	1.17	1.17	0.36
Sb	0.59	0.59	0.00	1.20	0.91	0.47
Bi	0.40	0.40	0.00	2.38	2.11	1.16

decay with the surface oxygen concentration η from f_0 to zero at the critical concentration η_c equivalent to the oxygen density in the X_2O_3 phase.

$$f(\eta) = f_0 e^{-\frac{\eta}{\eta_c - \eta}}. \quad (6)$$

Given such oxidation rate, the reaction time needed for the system to oxidize one cm^2 from oxygen concentration zero up to η is

$$T = 2 \int_0^\eta [f(x)]^{-1} dx. \quad (7)$$

In Fig. 4, we display the reaction time as a function of the relative O concentration η/η_c , for different temperatures. Here we can see a fast oxidation process for the FS systems. Indeed, experimental results on multilayer pnictogen systems have shown a fast oxidation process on the exposed surface layer [13–15]. However, on supported SiC systems, the time scale increases by several orders of magnitude. For As and Sb systems, despite the increased time scale, the oxidation process still hinders experimental realization of Arsenene/Antimonene at atmospheric

conditions. On the other hand, supported Bi present an oxidation process slow enough to allow an exposition of its surface on atmospheric condition. Increasing the temperature can lead to an oxidation reaction time drastically reduced. For instance, temperatures about 390 K should be enough for the supported Bi system to lose its oxidation robustness.

In summary, we have shown the triplet-singlet spin-transition of O_2 molecule, rules the oxidation process in monolayer pnictogens. Through our Landau-Zener statistical analysis, we have shown that the FS systems present higher spin-transition probabilities than the SiC-supported ones. By exploring the minimum energy path through the O_2 dissociation, we have extracted the barrier transition energy, compatible with our spin-transition analysis. Besides, spin-orbit coupling plays an important role in the oxidation mechanisms and time scales. Particularly, it has a significant effect on SiC-supported systems. The energy barrier presents an inverse dependence with the heavier pnictogen for the FS system (lower for Bi), while a direct dependence is observed for the SiC-supported systems (higher for Bi). The computed barriers confirm the enhanced robustness against oxidation for the SiC-supported systems. Based on that, we have established that according to the reaction time scale for complete oxidation (at 300 K), SiC-supported Bi is robust against atmospheric conditions. Our results open a path to explore the optimal 2D systems/substrate interplay aiming their experimental manipulation for further applications at atmospheric conditions.

ACKNOWLEDGMENTS

The authors acknowledge financial support from the Brazilian agencies FAPESP (grants 20/14067-

3, 19/20857-0, and 17/02317-2), CNPq, INCT-Nanocarbono, INCT-Materials Informatics, and Laboratório Nacional de Computação Científica for computer time (project ScafMat2 and emt2D).

-
- * rafael.freire@lnnano.cnpem.br
† felipe.lima@ilum.cnpem.br
‡ adalberto.fazzio@ilum.cnpem.br
- ¹ F. Reis, G. Li, L. Dudy, M. Bauernfeind, S. Glass, W. Hanke, R. Thomale, J. Schäfer, and R. Claessen, “Bismuthene on a SiC substrate: A candidate for a high-temperature quantum spin Hall material,” *Science* **357**, 287–290 (2017).
 - ² Fernando Dominguez, Benedikt Scharf, Gang Li, Jörg Schäfer, Ralph Claessen, Werner Hanke, Ronny Thomale, and Ewelina M. Hankiewicz, “Testing topological protection of edge states in hexagonal quantum spin Hall candidate materials,” *Phys. Rev. B* **98**, 161407 (2018).
 - ³ Ya ping Wang, Chang wen Zhang, Wei xiao Ji, Run wu Zhang, Ping Li, Pei ji Wang, Miao juan Ren, Xin lian Chen, and Min Yuan, “Tunable quantum spin Hall effect via strain in two-dimensional arsenene monolayer,” *Journal of Physics D: Applied Physics* **49**, 055305 (2016).
 - ⁴ Gul Rahman, Asad Mahmood, and Víctor M. García-Suárez, “Dynamically Stable Topological Phase of Arsenene,” *Scientific Reports* **9**, 7966 (2019).
 - ⁵ Bruno Focassio, Gabriel R. Schleder, Marcio Costa, Adalberto Fazzio, and Caio Lewenkopf, “Structural and electronic properties of realistic two-dimensional amorphous topological insulators,” *2D Materials* **8**, 025032 (2021).
 - ⁶ Armando Pezo, Bruno Focassio, Gabriel R. Schleder, Marcio Costa, Caio Lewenkopf, and Adalberto Fazzio, “Disorder effects of vacancies on the electronic transport properties of realistic topological insulator nanoribbons: The case of bismuthene,” *Phys. Rev. Mater.* **5**, 014204 (2021).
 - ⁷ Matthew J. Gilbert, “Topological electronics,” *Communications Physics* **4**, 70 (2021).
 - ⁸ J C Alvarez-Quiceno, R H Miwa, G M Dalpian, and A Fazzio, “Oxidation of free-standing and supported borophene,” *2D Materials* **4**, 025025 (2017).
 - ⁹ A. Ziletti, A. Carvalho, D. K. Campbell, D. F. Coker, and A. H. Castro Neto, “Oxygen Defects in Phosphorene,” *Phys. Rev. Lett.* **114**, 046801 (2015).
 - ¹⁰ Yu Guo, Si Zhou, Yizhen Bai, and Jijun Zhao, “Oxidation Resistance of Monolayer Group-IV Monochalcogenides,” *ACS Applied Materials & Interfaces* **9**, 12013–12020 (2017).
 - ¹¹ Siu-Pang Chan, Gang Chen, X. G. Gong, and Zhi-Feng Liu, “Oxidation of Carbon Nanotubes by Singlet O₂,” *Phys. Rev. Lett.* **90**, 086403 (2003).
 - ¹² W. Orellana, Antônio J. R. da Silva, and A. Fazzio, “O₂ Diffusion in SiO₂: Triplet versus Singlet,” *Phys. Rev. Lett.* **87**, 155901 (2001).
 - ¹³ Jianping Ji, Xiufeng Song, Jizi Liu, Zhong Yan, Chengxue Huo, Shengli Zhang, Meng Su, Lei Liao, Wenhui Wang, Zhenhua Ni, Yufeng Hao, and Haibo Zeng, “Two-dimensional antimonene single crystals grown by van der Waals epitaxy,” *Nature Communications* **7**, 13352 (2016).
 - ¹⁴ Pablo Ares, Fernando Aguilar-Galindo, David Rodríguez-San-Miguel, Diego A. Aldave, Sergio Díaz-Tendero, Manuel Alcamí, Fernando Martín, Julio Gómez-Herrero, and Félix Zamora, “Mechanical Isolation of Highly Stable Antimonene under Ambient Conditions,” *Advanced Materials* **28**, 6332–6336 (2016).
 - ¹⁵ Mhamed Assebban, Carlos Gibaja, Michael Fickert, Iñigo Torres, Erik Weinreich, Stefan Wolff, Roland Gillen, Janina Maultzsch, Maria Varela, Sherman Tan Jun Rong, Kian Ping Loh, Enrique G Michel, Félix Zamora, and Gonzalo Abellán, “Unveiling the oxidation behavior of liquid-phase exfoliated antimony nanosheets,” *2D Materials* **7**, 025039 (2020).
 - ¹⁶ Shengli Zhang, Shiyang Guo, Zhongfang Chen, Yeliang Wang, Hongjun Gao, Julio Gómez-Herrero, Pablo Ares, Félix Zamora, Zhen Zhu, and Haibo Zeng, “Recent progress in 2D group-VA semiconductors: from theory to experiment,” *Chem. Soc. Rev.* **47**, 982–1021 (2018).
 - ¹⁷ Martin Pumera and Zdeněk Sofer, “2D Monoelemental Arsenene, Antimonene, and Bismuthene: Beyond Black Phosphorus,” *Advanced Materials* **29**, 1605299 (2017).
 - ¹⁸ Andrey A Kistanov, Yongqing Cai, Kun Zhou, Sergey V Dmitriev, and Yong-Wei Zhang, “The role of H₂O and O₂ molecules and phosphorus vacancies in the structure instability of phosphorene,” *2D Materials* **4**, 015010 (2016).
 - ¹⁹ Andrey A. Kistanov, Yongqing Cai, Devesh R. Kripalani, Kun Zhou, Sergey V. Dmitriev, and Yong-Wei Zhang, “A first-principles study on the adsorption of small molecules on antimonene: oxidation tendency and stability,” *J. Mater. Chem. C* **6**, 4308–4317 (2018).
 - ²⁰ Andrey A. Kistanov, Salavat Kh. Khadiullin, Kun Zhou, Sergey V. Dmitriev, and Elena A. Korznikova, “Environmental stability of bismuthene: oxidation mechanism and structural stability of 2D pnictogens,” *J. Mater. Chem. C* **7**, 9195–9202 (2019).
 - ²¹ Andrey A. Kistanov, Salavat Kh. Khadiullin, Sergey V. Dmitriev, and Elena A. Korznikova, “A First-Principles Study on the Adsorption of Small Molecules on Arsenene: Comparison of Oxidation Kinetics in Arsenene, Antimonene, Phosphorene, and InSe,” *ChemPhysChem* **20**, 575–580 (2019).
 - ²² Salavat Kh. Khadiullin, Andrey A. Kistanov, Svetlana V. Ustiuzhanina, Artur R. Davletshin, Kun Zhou, Sergey V. Dmitriev, and Elena A. Korznikova, “First-Principles Study of Interaction of Bismuthene with Small Gas Molecules,” *ChemistrySelect* **4**, 10928–10933 (2019).
 - ²³ Salavat Khadiullin, Artur Davletshin, Kun Zhou, and Elena Korznikova, “Analysis of Chemical Activity of Bismuthene in the Presence of Environment Gas Molecules by Means of Ab Initio Calculations,” in *TMS 2020 149th Annual Meeting & Exhibition Supplemental Proceedings* (Springer International Publishing, Cham, 2020) pp. 983–991.
 - ²⁴ Yan Shao, Zhong-Liu Liu, Cai Cheng, Xu Wu, Hang Liu, Chen Liu, Jia-Ou Wang, Shi-Yu Zhu, Yu-Qi Wang, Dong-Xia Shi, Kurash Ibrahim, Jia-Tao Sun, Ye-Liang Wang, and Hong-Jun Gao, “Epitaxial Growth of Flat Antimonene

- Monolayer: A New Honeycomb Analogue of Graphene,” *Nano Letters* **18**, 2133–2139 (2018), PMID: 29457727.
- 25 F. Reis, G. Li, L. Dudy, M. Bauernfeind, S. Glass, W. Hanke, R. Thomale, J. Schäfer, and R. Claessen, “Bismuthene on a SiC substrate: A candidate for a high-temperature quantum spin Hall material,” *Science* **357**, 287–290 (2017).
 - 26 Anderson K. Okazaki, Rafael Furlan de Oliveira, Rafael Luiz Heleno Freire, Adalberto Fazzio, and Felipe Crasto de Lima, “Uncovering the Structural Evolution of Arsenene on SiC Substrate,” *The Journal of Physical Chemistry C* **127**, 7894–7899 (2023).
 - 27 Peiwen Yuan, Teng Zhang, Jiatao Sun, Liwei Liu, Yugui Yao, and Yeliang Wang, “Recent progress in 2D group-V elemental monolayers: fabrications and properties,” *Journal of Semiconductors* **41**, 081003 (2020).
 - 28 Zhuhua Zhang, Jun Yin, Xiaofei Liu, Jidong Li, Jiahuan Zhang, and Wanlin Guo, “Substrate-Sensitive Graphene Oxidation,” *The Journal of Physical Chemistry Letters* **7**, 867–873 (2016).
 - 29 P. Hohenberg and W. Kohn, “Inhomogeneous Electron Gas,” *Phys. Rev.* **136**, B864–B871 (1964).
 - 30 W. Kohn and L. J. Sham, “Self-consistent equations including exchange and correlation effects,” *Phys. Rev.* **140**, A1133–A1138 (1965).
 - 31 J. P. Perdew, K. Burke, and M. Ernzerhof, “Generalized gradient approximation made simple,” *Phys. Rev. Lett.* **77**, 3865–3868 (1996).
 - 32 P. E. Blöchl, “Projector augmented-wave method,” *Phys. Rev. B* **50**, 17953–17979 (1994).
 - 33 G. Kresse and D. Joubert, “From ultrasoft pseudopotentials to the projector augmented-wave method,” *Phys. Rev. B* **59**, 1758–1775 (1999).
 - 34 G. Kresse and J. Hafner, “Ab Initio Molecular Dynamics for Open-Shell Transition Metals,” *Phys. Rev. B* **48**, 13115–13126 (1993).
 - 35 G. Kresse and J. Furthmüller, “Efficient iterative schemes for ab initio total-energy calculations using a plane-wave basis set,” *Phys. Rev. B* **54**, 11169–11186 (1996).
 - 36 Clarence Zener and Ralph Howard Fowler, “Non-adiabatic crossing of energy levels,” *Proceedings of the Royal Society of London. Series A, Containing Papers of a Mathematical and Physical Character* **137**, 696–702 (1932).
 - 37 Jeremy N. Harvey, “Understanding the kinetics of spin-forbidden chemical reactions,” *Phys. Chem. Chem. Phys.* **9**, 331–343 (2007).
 - 38 Jeremy N. Harvey, “Spin-forbidden reactions: computational insight into mechanisms and kinetics,” *WIREs Computational Molecular Science* **4**, 1–14 (2014).
 - 39 Jörg Behler, Bernard Delley, Sönke Lorenz, Karsten Reuter, and Matthias Scheffler, “Dissociation of O_2 at $\text{Al}(111)$: The role of spin selection rules,” *Phys. Rev. Lett.* **94**, 036104 (2005).